Monte Carlo Technique for the Determination of Thermal Radiation Shape Factors

S. J. Hoff, STUDENT MEMBER ASAE
K. A. Janni, ASSOC. MEMBER ASAE

ABSTRACT

The principles and equations of the Monte Carlo technique are outlined for determining thermal radiation shape factors. Equations for the ray tracings and intersection criteria needed to calculate the shape factors between plane walls, cylinders and spheres are presented. The equations presented and resulting shape factors are demonstrated with selected geometric configurations for which the shape factors are known. Computer results using the Monte Carlo technique of six geometric arrangements produced results within 2.2% of theoretically known shape factors.

INTRODUCTION

Many energy balances encountered in thermal engineering problems require the determination of the radiative heat transfer. Computationally, radiation heat transfer can become quite cumbersome for two reasons. First, the radiative component is dependent on the fourth power of the surface temperature. This, combined with the first power temperatures associated with convection and conduction, result in a nonlinear analysis. Second, unlike the convective and conductive heat loss components, the radiative component depends on shape factors which are a function of the spatial orientation between surfaces.

Shape factors are defined as the fraction of radiant energy leaving one surface that is incident upon another. Shape factors are known for a few common shapes and geometric orientations, however, many situations exist where shape factors are unknown. For these situations, alternate techniques must be used to numerically estimate them.

One technique, called the Monte Carlo method, is a statistical model which simulates the radiative emission from a surface. The Monte Carlo technique is commonly used to describe the complete radiative exchange (Howell, 1965; Weiner et al., 1965; Toor and Viskanta, 1968). For this analysis, the Monte Carlo technique was only used to calculate shape factors. Once shape factors are known, a complete energy exchange, including conduction and convection, can be computed using an energy balance and solution procedure presented in Hoff (1987).

This paper describes the Monte Carlo technique for determining shape factors between gray-body surfaces that are both diffuse emitters and reflectors of radiant energy and where the radiosity (total radiative outflow) is uniform throughout the surface. The objective is to present and verify the equations and intersection criteria which simulate the radiant emission and reflection (ray equations) from plane walls, cylinders and spheres. Several geometric arrangements involving planes, cylinders and spheres were analyzed to compare the Monte Carlo results with theoretically known shape factors. The ray equations, once verified, can be used to calculate the shape factors of more complicated geometries by combining these basic shapes.

MONTE CARLO TECHNIQUE

The Monte Carlo technique for estimating shape factors begins with a mathematical description of the radiative emission from a surface. For diffuse surfaces, the emission from a surface is assumed to include the emitted energy and the reflected energy from all other surfaces in an enclosure incident upon the surface. The Monte Carlo technique randomly generates values for all variables that affect the diffuse emission and reflection of radiant energy. These values are used to simulate the theoretically known distribution of radiant emission. The resulting distribution of energy is used to estimate the shape factor from one surface to another.

The three principle variables that affect the distribution of diffuse radiant emission are wavelength (λ), cone angle (θ) and azimuth angle (ϕ) (Fig. 1a). For assumed gray-body surfaces, the total emissivity is equal to the total absorbtivity which implies that the emissive characteristics of a surface are independent of the wavelength. Another common assumption (Siegal and Howell, 1978) is that the emitted and reflected radiation are independent of the azimuth angle. This implies that each azimuth angle (0 to 360°) has an equal probability of occurring. The only remaining variable to be considered in the emitted energy function is the cone angle.

To determine the distribution of the emitted and reflected radiation as a function of the cone angle, the mathematical description of emitted radiation from a surface as a function of the cone angle must be defined. The complete development can be found in Siegel and Howell (1978). For any surface i, the total emitted energy

Article was submitted for publication in May 1988; reviewed and approved for publication by the Structures and Environment Div. of ASAE in February 1989.

Published as Paper No. 15,784 of the Scientific Journal Series of the Minnesota Agricultural Experiment Station on research conducted under Minnesota Agricultural Experiment Project No. 12-076.

The authors are: S. J. HOFF, Graduate Research Assistant and K. A. JANNI, Associate Professor, Agricultural Engineering Dept., University of Minnesota, St. Paul.

  0001-2351/89/3203-1023$03.00

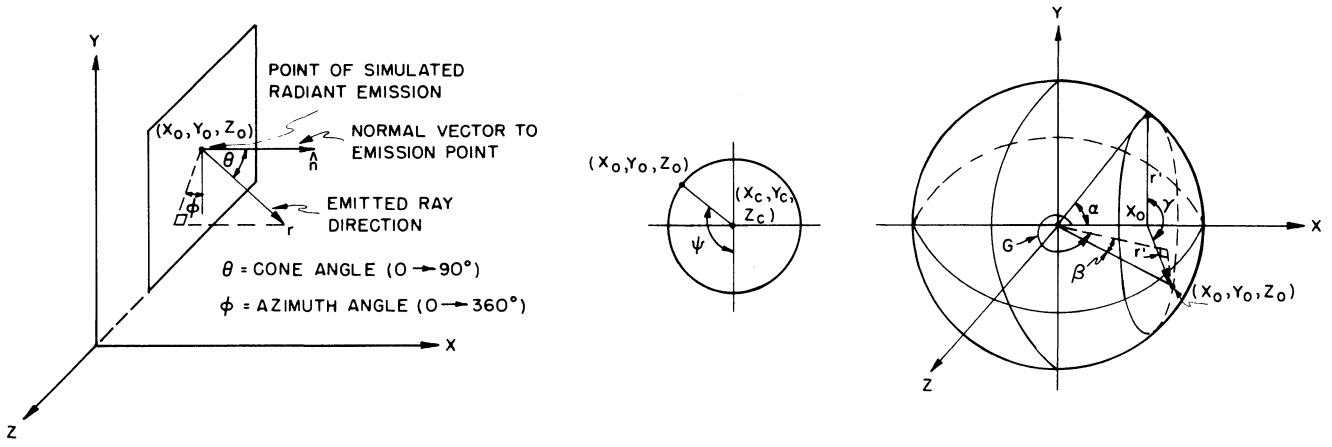

(a) (b) (c)

Fig. 1—Angle references used to describe emission rays and emission points.

per unit time is (see nomenclature for variable definition):

$$dQ_{e,i} = \epsilon_i(T)\, \sigma T_i^4\, dA_i \quad \ldots\ldots\ldots\ldots\ldots\ldots [1]$$

where

$$\epsilon_i(T) = \frac{[I'_{b,i} \int_\omega \epsilon'_i(\theta,T) \cos\theta_i\, d\omega]}{\sigma T_i^4} \quad \ldots\ldots\ldots [2]$$

The energy emitted by element dA_i per unit time in the interval $d\theta_i$ about θ_i is:

$$d^2Q_{e,i}(\theta_i) = 2\pi\, \epsilon'_i(\theta, T)\, I'_{b,i}(T) \cos\theta_i\, dA_i \sin\theta_i\, d\theta_i$$

$$\ldots\ldots\ldots\ldots\ldots\ldots\ldots\ldots\ldots\ldots\ldots\ldots [3]$$

Thus, the probability of radiant emission in any one cone angle direction θ_i can then be expressed as:

$$P(\theta_i)\, d\theta_i = \frac{d^2\, Q_{e,i}(\theta_i)}{dQ_{e,i}} \quad \ldots\ldots\ldots\ldots\ldots [4]$$

Substituting the previously defined terms, inserting the definition of the black-body intensity ($I'_{bi} = \sigma T_i 4/\pi$) and recognizing that for diffuse surfaces the emissivity is independent of the cone angle, θ_i, results in the probability density function:

$$P(\theta_i) = 2 \cos\theta_i \sin\theta_i \quad \ldots\ldots\ldots\ldots\ldots [5]$$

This function describes the theoretical distribution of radiant emission from a diffuse-gray surface as well as the distribution of reflected energy incident upon the surface from all other surfaces in the enclosure. The random selections of θ_i used must match this density function, which can be accomplished by utilizing the cumulative distribution of the probability density function (Siegel and Howell, 1978). The cumulative distribution of equation [5] is by definition the integrated probability density function from 0 to $\pi/2$ radians and has a value of 1. If a random number, R_θ, is chosen between 0 and 1 (inclusive), then the corresponding value of the cone angle can be determined by integrating equation [5]. Mathematically, this becomes:

$$R_\theta = \int_{\theta_i} P(\theta_i)\, d\theta_i = \int_{\theta_i} 2 \cos\theta_i \sin\theta_i\, d\theta_i \quad \ldots\ldots [6]$$

and solving in terms of the cone angle becomes:

$$R_\theta = \sin^2\theta_i \quad \ldots\ldots\ldots\ldots\ldots\ldots\ldots [7]$$

Solving for the cone angle yields the desired result:

$$\theta_i = \sin^{-1}(R_\theta)^{0.5} \quad \ldots\ldots\ldots\ldots\ldots\ldots [8]$$

The azimuth angle, for which radiant emission and reflection were assumed independent, becomes:

$$\phi_i = 2\pi R_\phi \quad \ldots\ldots\ldots\ldots\ldots\ldots\ldots [9]$$

The Monte Carlo procedure is to select two random numbers (R_θ and R_ϕ) and calculate the cone and azimuth angles from each using equations [8] and [9], respectively. After the emission angles are determined, the complete direction of an emitted ray can be traced mathematically to a surface of incidence. By definition then, the shape factor is the amount of energy leaving one surface that is incident on another. Using this technique, the shape factor from surface i to n can be calculated as:

$$F_{i-n} = \frac{\text{rays incident on surface n}}{\text{total rays emitted from surface i}} \quad \ldots\ldots [10]$$

SHAPE FACTOR DETERMINATION

The procedure to find the shape factors, once the emission angles are determined, is to trace the emitted ray from the surface of origin to all surfaces of intersection. The surfaces which are intersected are recorded and the surface corresponding to the shortest ray length becomes the surface of incidence for that ray.

The governing ray equations for an emitted ray originating from a plane wall, cylinder or sphere are outlined in Table 1. The equations and angle references (Figs. 1a to 1c)specify the emitted ray coordinates. The conditions necessary to identify valid surface intersections are outlined as follows.

TABLE 1. Governing Emission Ray Equations for Plane Wall, Cylinder and Sphere

Emission Surface	Governing Ray Equations	Equation Set
Plane Wall Located at x=0	$x = x_o + r\cos\theta \quad (x_o = 0)$ $y = y_o - r\sin\theta\cos\phi$ $z = z_o + r\sin\theta\sin\phi$	[1]
Cylinder with Axis Parallel to x=0 Plane	$x = x_o + r\cos\theta\sin(360-\psi) + r\sin\theta\cos E\cos(360-\psi)$ $y = y_o - r\cos\theta\cos(360-\psi) + r\sin\theta\cos E\sin(360-\psi)$ $z = z_o - r\sin\theta\sin\phi$ where; $x_o = x_c - r_c\sin\psi$ $y_o = y_c - r_c\cos\psi$ z_o = pre-selected and; $E = \phi$ if $\psi <= 180$ $= 180 + \phi$ if $\psi > 180$	[2]
Sphere	$x = x_o + r\cos\theta\cos\beta\cos G - r\sin\theta\sin\phi\sin G + r\sin\theta\cos\phi\sin\beta\cos G$ $y = y_o + r\cos\theta\sin\beta - r\sin\theta\cos\phi\cos\beta$ $z = z_o - r\cos\theta\cos\beta\sin G - r\sin\theta\sin\phi\cos G - r\sin\theta\cos\phi\sin\beta\sin G$ where; x_o = pre-selected $y_o = y_c + r_s\sin\alpha\cos\gamma$ $z_o = z_c - r_s\sin\alpha\sin\gamma$ $\beta = \sin^{-1}((y_o - y_c)/r_s)$ $\xi = \tan^{-1}((z_c - z_o)/(x_o - x_c))$ and; $G = \xi$ if $z_o < z_c$ and $x_o > x_c$ $= \xi+\pi$ if $z_o \leq z_c$ and $x_o < x_c$ $= \xi+\pi$ if $z_o > z_c$ and $x_o < x_c$ $= \xi+2\pi$ if $z_o > z_c$ and $x_o > x_c$ $= \pi/2$ if $z_o = z_c$ and $x_o = x_c$	[3]

Plane Wall Intersection

The intersection of a ray onto a plane wall is straight forward since the equation describing this surface is readily known. The intersection test requires the substitution of the plane equation into the appropriate governing ray equations from Table 1. Given the x, y and z coordinates of the emitted ray, the equations can be solved for the ray length, r, corresponding to the point of intersection. The remaining two equations are then solved for the remaining two intersection coordinate dimensions.

For example, assume that the emission surface is a plane located at x=0 and that the plane located at y=0 is to be tesed for intersection. Furthermore, assume that ϕ=0, θ=45, y_o=1.5 and z_o=-1.5. From the governing ray equations (Table 1, equation set 1), the length of the ray which intersects the y=0 plane is 2.12, and the x and z dimensions of the intersecting point become 1.5 and -1.5, respectively. If the point (1.5, 0, -1.5) lies within the dimensions of the plane located at y=0, then the intersection point is valid.

Cylinder Intersection

The intersection of a cylinder requires that the governing ray coordinates of an emitted ray must satisfy the circle which defines the circumferential boundary of the cylinder. The circle equation that forms a cylinder parallel to the x=0 plane is;

$$(x - x_c)^2 + (y - y_c)^2 = r_c^2 \quad \ldots\ldots\ldots\ldots\ldots\ldots [11]$$

The x and y coordinates of the emitted ray are substituted into this equation and solved for the ray length of intersection. For example, if the shape factor between a plane wall located at x=0 and a cylinder parallel to this plane is desired, a quadratic equation for the ray length results, where;

$$r = \frac{-b - \sqrt{b^2 - 4ac}}{2a} \quad \ldots\ldots\ldots\ldots\ldots\ldots [12]$$

where

$a = \cos^2\theta + \sin^2\theta\cos^2\phi$

$b = 2y_c\sin\theta\cos\phi - 2X_c\cos\theta - 2y_o\sin\theta\cos\phi$

$c = y_c^2 + X_c^2 + y_c^2 - 2y_cy_o - r_c^2$

A valid intersection is found if the root is real and the ray length, r, is greater than 0. If a valid intersection is found, the z coordinate of the intersection point is calculated and if within the bounds (length) of the cylinder, an accepted surface intersection is recorded.

Spherical Intersection

The spherical intersection follows in the same manner as the cylinder intersection outlined. Given the same plane wall emission at x=0 situation, the conditions necessary for a valid intersection are;

$$r = \frac{-b - \sqrt{b^2 - 4ac}}{2a} \quad \ldots\ldots\ldots\ldots\ldots\ldots [13]$$

where

$a = 1.0$

$b = \sin\theta\cos\phi(2y_c - 2y_o) + \sin\theta\sin\phi(2z_o - 2z_c) - 2x_c\cos\theta$

$c = x_c^2 + y_c^2 + z_c^2 + y_o^2 + z_o^2 - 2y_cy_o - 2z_oz_c - r_s^2$

Grid Spacing for Emitting Surfaces

In general, the emitting surface must be divided into sufficiently small grids. For the plane wall emissions, the grid spacing used was 0.03 m in both the y and z dimension. For the cylinder emissions, the grid spacing used was every $\pi/24$ radians around the cylinder (ψ) and every 0.03 m along its axis. Finally, for the sphere emissions, the x-axis of the sphere was divided equally at x_o = 0.05 m segments, and at each of these points, rays were emitted every $\pi/24$ radians (γ) perpendicular to the x-axis. For all three emission surface examples given, 21 rays were emitted per point. The selected grid spacings and emission rays per emission point were selected after extensive numerical experiments indicated that these values gave error deviations less than 3%, which was arbitrarily selected as the acceptable limit.

Computer Implementation

Four computer programs were written to simulate the shape factors between plane-walls, a cylinder and a

TABLE 2. Monte Carlo vs. Theoretical - Selected Geometric Arrangements

Geometric Set-up	Shape Factor	Emitted Rays	Density (rays/m^2)	Monte Carlo	Theo-retical	% Error
Plane Wall Enclosure (Case 1, Fig. 1a)	F_{2-1}	196,000	33,300	0.1259	0.1248	+0.9
	F_{2-2}			0.0000	0.0000	0
	F_{2-3}			0.1224	0.1248	−1.9
	F_{2-4}			0.3239	0.3213	+0.8
	F_{2-5}			0.2104	0.2145	−1.9
	F_{2-6}			0.2174	0.2145	+1.4
Plane Wall to Cylinder of Same Length (Case 2, Fig. 1b)	F_{2-1}	reciprocity employed		0.2167	0.2189	−1.0
Cylinder to Plane Wall (Case 3, Fig. 1c)	F_{1-2}	31,250	415	0.1380	0.1394	−1.0
Sphere to Circle (Case 4, Fig. 1c)	F_{s-1}	161,280	3,210	0.0710	0.0713	−0.4
Sphere to Plane Wall Enclosure (Case 5, Fig. 1d)	F_{s-1}	161,280	3,210	0.1640	0.1667	−1.6
	F_{s-2}			0.1653	0.1667	−0.8
	F_{s-3}			0.1671	0.1667	+0.2
	F_{s-4}			0.1703	0.1667	+2.2
	F_{s-5}			0.1675	0.1667	+0.5
	F_{s-6}			0.1658	0.1667	−0.5
Plane Wall to Sphere (Case 6, Fig. 1d)	F_{2-s}	49,400	494	0.0851	0.0855	−0.5

plane-wall, a sphere and a plane-wall, and a plane-wall and a sphere. The shape factor between a plane-wall and a cylinder was calculated using reciprocity from the results generated for the shape factor between a cylinder and a plane-wall (Table 2). All simulations were generated using FORTRAN programs on an IBM XT Model 286. The two random numbers generated (R_θ and R_ϕ) for each emitted ray were calculated using the linear congruential method (Knuth, 1973).

RESULTS AND DISCUSSION

A comparison of shape factors estimated using the Monte Carlo technique versus theoretically known values is presented in Table 2. The geometric orientations used (Figs. 2a to 2d) were a six-sided plane-wall enclosure (case 1), a plane-wall to a cylinder (case 2), a cylinder to a plane-wall (case 3), a sphere to a plane-wall (cases 4 and 5) and a plane-wall to a sphere (case 6). Total computer running time (real time) varied from approximately four min for case 3 to 20 min for cases 1, 4 and 5.

All of the estimated shape factors in Table 2 were within 2.2% of the theoretically known values. The largest error occurred in the emission from a sphere to a plane wall (case 5) in which the predicted shape factor was 0.1703 compared to the theoretical value 0.1667. Ironically, the smallest error recorded in Table 2 also

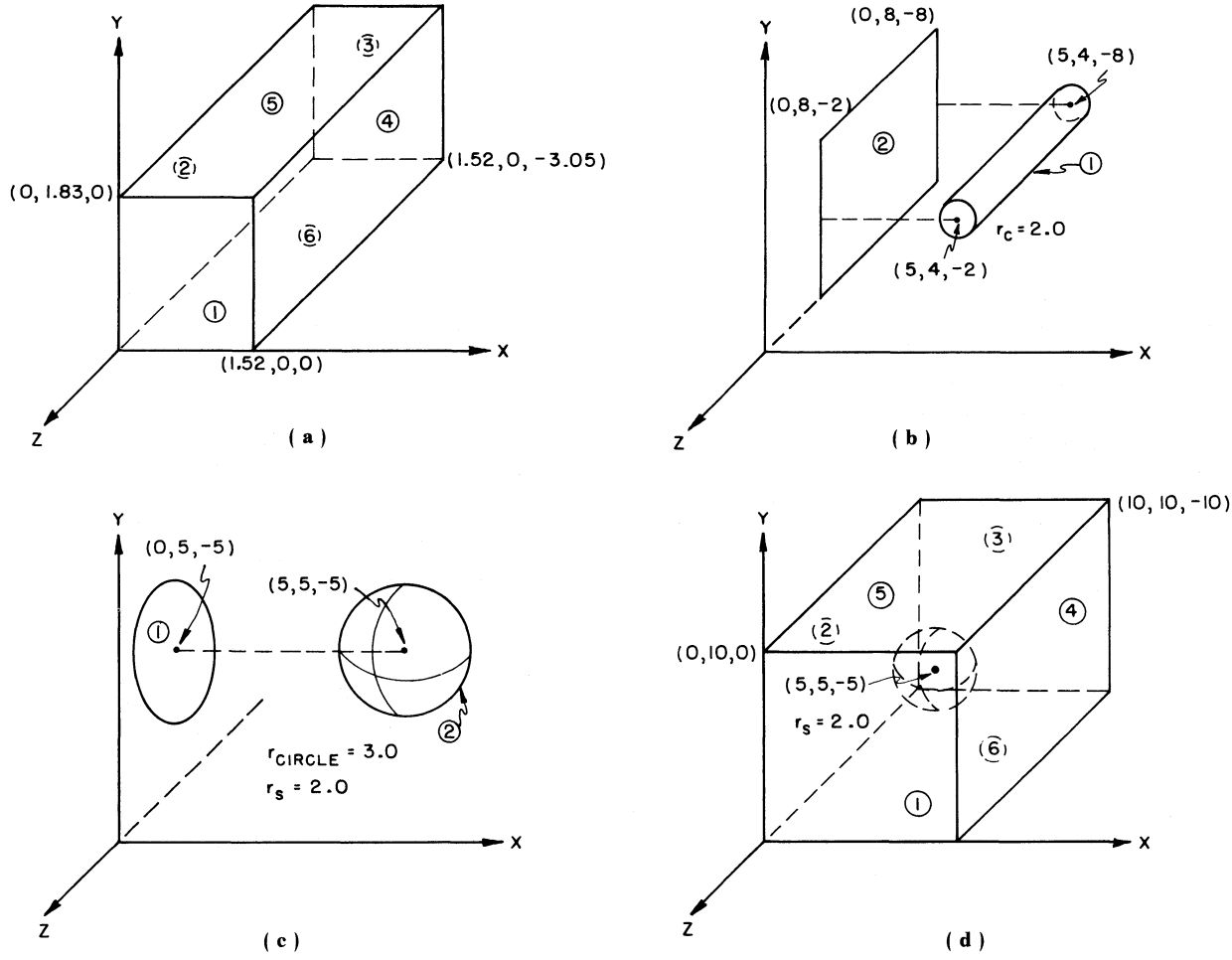

Fig. 2—Geometric arrangements used to verify the Monte Carlo technique (all units in meters).

TABLE 3. Emission Ray Sample Size vs. Percent Error Deviation from Theoretical - Case 3

Grid Configuration*					
Z-Axis Interval (m)	Emission Rays per Emission Point	Sample Size (rays)	Density (rays/m^2)	|%Error|	Average %Error (S.D.)
1.0	2	672	9	5.0	
1.0	6	2016	27	5.0	4.5
1.0	11	3696	49	4.9	(1.0)
1.0	21	7056	94	2.9	
0.5	2	1248	17	9.8	
0.5	6	3744	50	3.3	4.6
0.5	11	6864	91	0.1	(4.1)
0.5	21	13104	174	5.1	
0.2	2	2880	38	0.4	
0.2	6	8640	115	0.2	0.5
0.2	11	15840	210	0.3	(0.4)
0.2	21	30240	401	1.1	
0.1	2	5856	78	0.2	
0.1	6	17568	233	0.3	0.4
0.1	11	32208	427	0.8	(0.3)
0.1	21	61488	816	0.4	

* circumferential grid spacing constant at π / 24 radians

occurred for the emission from a sphere to a plane wall (case 5) in which the predicted shape factor was 0.1671 compared to the known result of 0.1667. These oscillations about the theoretical shape factor have been described before (Howell, 1965) and are the result of the statistical nature of the Monte Carlo technique. Suggested remedies are to average the resulting shape factors over several numerical simulations. This averaging process was not performed for the results presented.

The deviation from the known result remained fairly constant for all cases even though the total ray emissions and subsequent emission densities varied substantially for each emitting surface. For example, in case 1 an emission density of 33,000 rays/m^2 was used, whereas no more than 3,210 rays/m^2 were used for cases 2 thru 6. This reduction in emission density by 90% did not increase the error of the predicted shape factors. The fact that a large sample size resulting in a large emission density did not necessarily guarantee a more accurate result required further analysis.

Grid Size and Emission Density

Emission ray sample size and density is a function of both the grid size and the number of emission rays per emission point. Table 3 shows the percent error in the predicted shape factors for case 3 obtained using various grid sizes and number of emission rays per point. The emission ray density ranged from 9 to 816 rays/m^2.

The grid spacing was varied from 1.0 to 0.1 m along the z-axis of the cylinder (Fig. 2b). The circumferential spacing was held constant at $\psi = \pi/24$ radians. The average error for each z-axis interval ranged from 4.6% using a 0.5 m interval to 0.4% with a 0.1 m interval.

The number of emission rays per point was varied from 2 to 21 rays. At a z-axis interval of 1.0 m the smallest percent error was 2.9% using 21 rays per point. At the 0.5 m interval the smallest error occurred using 11 rays per point. The smallest errors at 0.2 and 0.1 m intervals occurred at 6 and 2 rays per point, respectively. This shows that increasing the number of emission rays per grid point does not necessarily increase the accuracy of the predicted shape factors. A relatively small grid spacing is required to produce accurate shape factor estimates.

The grid spacing used for the six cases, which resulted in all the shape factors having less than 3% error, can be analyzed in terms of dimensionless values. For the plane wall emissions (case 1), the dimensionless grid spacing ($\Delta L/L$) was 0.016 and 0.010 for the y and z directions, respectively. For cylinder emissions (case 3), the dimensionless spacing along the z-axis was 0.005 and for the sperical emissions (case 5), the dimensionless spacing ($\Delta x/r_s$) was 0.025. Therefore, dimensionless grid spacings between 0.005 and 0.025 resulted in shape factors within 3% of theoretical. Given the constant circumferential spacings of $\pi/24$ radians (cylinder and spherical emissions) and the constant sample size of 21 emitted rays per emission point, the general recommendation from this study would be to maintain the dimensionless grid spacing less than 0.025.

The grid spacing guidelines are approximations at best. For each geometric configuration encountered, several numerical experiments should be performed and the resulting average shape factor used.

It is essential that the surface-area weighted emission ray density be uniform throughout the entire surface. If this is not achieved, a different number of rays will be emitted for one section of the surface, invalidating the uniform radiosity assumption prescribed at the outset.

CONCLUSIONS

The Monte Carlo technique was demonstrated for determining shape factors between plane walls, cylinders and spheres. The surfaces were both gray and diffuse emitters and reflectors of radiant energy and of uniform radiosity throughout. From the results presented, the following conclusions can be drawn;

1. The Monte Carlo technique can be used to estimate the thermal radiation shape factors between plane-walls, cylinders and spheres using simple computer programming techniques.
2. Resulting shape factors using the Monte Carlo technique and the presented ray equations for various orientations between plane-walls, cylinders and spheres were all within 2.2% of the theoretically calculated values.
3. Varying the sample size through adjustments in grid spacing intervals and emission levels per emission point indicated that a relatively small grid spacing interval is of greater importance in predicting the shape factor than the number of emitted rays. Total sample size is of little importance without a uniformly small grid spacing.

References

1. Hoff, S. J. 1987. Effect of hovers on the radiative and convective heat loss from a modelled new-born piglet. M.S. thesis. University of Minnesota.

2. Howell, J. R. 1965. Calculation of radiant heat exchange by the Monte Carlo method. Paper No. 65-WA/HT-54. American Society of Mechanical Engineers.

3. Knuth, D. E. 1973. *Art of Computer Programming.* 2nd ed. Vol. 2. Reading, MA: Addison-Wesley Co.

4. Siegal, R. and J.R. Howell. 1978. *Thermal Radiation Heat Transfer.* 2nd ed. pp. 354-382. McGraw-Hill Book Co.

5. Toor, J. S. and R. Viskanta. 1968. A numerical experiment of radiant heat interchange by the Monte Carlo method. *International Journal of Heat and Mass Transfer* 11:883-897.

6. Weiner, M. M., J. W. Tindall and L. M. Candell. 1965. Radiative interchange factors by Monte Carlo. Paper No. 65-WA/HT-51. American Society of Mechanical Engineers.

NOMENCLATURE

A = surface area (m^2)
C = cumulative distribution
F = shape factor
I′ = black body radiant intensity (W/m^2)
P = probability density function
Q_e = total emitted radiant energy (W)
r = emitted ray length (m)
r_c = cylinder radius (m)
r_s = sphere radius (m)
R_θ = random number generated for the cone angle
R_ϕ = random number generated for the azimuth angle
T = temperature (C)
x,y,z = 3-dimensional coordinates (m)

Greek Symbols:

ε = total hemispherical emissivity
ε' = total directional emissivity
σ = Stefan-Boltzmann constant (5.6696×10^{-8} W/m^2-K^4)
θ = cone angle of emission (radians, Figure 1a)
ϕ = azimuth angle of emission (radians, Figure 1a)
ω = solid angle (radians)
ψ = circumferential cylinder angle (radians, Figure 1b)
α = z=0 plane spherical angle (radians, Figure 1c)
γ = circumferential sphere angle (radians, Figure 1c)

Subscripts

b = black-body
c = surface center
i,n = surface designation
o = emission ray origin